ISSN 1070-3284, Russian Journal of Coordination Chemistry, 2019, Vol. 45, No. 1, pp. 47–55. © Pleiades Publishing, Ltd., 2019.
Russian Text © N.V. Somov, F.F. Chausov, N.V. Lomova, R.M. Zakirova, I.V. Fedotova, V.G. Petrov, M.A. Shumilova, D.K. Zhirov, 2019, published in Koordinatsionnaya Khimiya, 2019, Vol. 45, No. 1, pp. 48–57.

Nitrilotris(methylenephosphonic) Complexes of Lanthanides $[Na(H_2O)_x]_2[Ln^{III}Na_6H(H_2O)_{10}\{N(CH_2PO_3)_3\}_2] \cdot nH_2O$ (Ln^{III} = Pr, Nd)

N. V. Somov[a, *], F. F. Chausov[b, c], N. V. Lomova[b], R. M. Zakirova[c], I. V. Fedotova[c], V. G. Petrov[b], M. A. Shumilova[b], and D. K. Zhirov[b]

[a] *Lobachevsky National Research University, Nizhny Novgorod, 603950 Russia*
[b] *Udmurt Federal Research Center, Ural Branch, Russian Academy of Sciences, Izhevsk, 426067 Russia*
[c] *Udmurt State University, Izhevsk, 426034 Russia*
**e-mail: somov@phys.unn.ru*

Received March 12, 2018; revised April 5, 2018; accepted June 15, 2018

Abstract—The sodium salts of lanthanide nitrilotris(mehylenephosphonate) complexes $[Na(H_2O)_x]_2[Ln^{III}Na_6H(H_2O)_{10}\{N(CH_2PO_3)_3\}_2] \cdot nH_2O$, where Ln^{III} = Pr (**I**), and Nd (**II**), were prepared, isolated, and studied. The isostructural crystals are monoclinic, space group $P2_1/c$, $Z = 2$; for complex **I**, $a = 11.8168(7)$, $b = 10.5403(9)$, $c = 19.8094(10)$ Å, $\beta = 94.232(5)°$; for complex **II**, $a = 11.7999(2)$, $b = 10.5495(2)$, $c = 19.7976(3)$ Å, $\beta = 94.158(2)°$. The lanthanide ions are coordinated at the center of a cage consisting of two $\{N(CH_2PO_3)_3\}$ acid residues and six sodium ions, which form P–O–Na–O–P bridges. The Ln coordination polyhedron is a regular rhombohedron (CIF files CCDC nos. 1825702 (**I**), 1825700 (**II**)).

Keywords: neodymium, praseodymium, coordination compounds, X-ray diffraction, IR spectroscopy, Raman spectroscopy, thermogravimetry

DOI: 10.1134/S107032841901010X

INTRODUCTION

The coordination compounds of lanthanides with N,O-ligands are the subjects of extensive research and have diverse applications. The lanthanide complexes with aminopolycarboxylic acids (complexones) are most studied [1–4] and are used in industrial lanthanide separation processes and in analytical chemistry as diagnostic contrast agents, luminophores, and so on.

A specific feature of N,O-coordinated lanthanide complexes, which distinguishes them from analogous compounds of most other elements, is the considerable difference between the M–N and M–O distances [5]. For complexes of most metals, the ⟨M–N⟩–⟨M–O⟩ value is 0.0–0.2 Å; meanwhile, the ⟨M–N⟩–⟨M–O⟩ values typical of *f*-elements are 0.3 Å and more [3, 5], which gives rise to assumption [6] of specific features involved in the coordination bonds of lanthanides. Whereas nitrogen has one lone pair (LP) of electrons and can form only a single coordination bond with the complexing metal atom, the O atom contains two LPs and can form a multiple coordination bond with the complexing metal atom. This occurs on coordination of lanthanides, especially light ones, which have a rather large number of vacant electron states in the valence band and rather large HOMO–LUMO gap [7], which accounts for the preferred complexation of lanthanides with hard ligands [8, 9].

Vivid examples of N,O-ligands are aminopolyphosphonic acids, in particular, nitrilo-tris(methylenephosphonic acid) $N(CH_2PO_3)_3H_6$ ($NTPH_6$), which can bind to metals in different fashions [10–18]. The NTP complexes with metals are used as corrosion inhibitors [19–21] and bactericides [22]. Complexes of some lanthanides with NTP show properties of proton conductors [23]. The complexes $Ln^{III}NTPH_3 \cdot nH_2O$ were comprehensively studied by I.V. Tananaev and co-workers [24]. According to spectroscopic data, the N atom of the NTP molecule in these complexes is protonated and is not involved in the bonding to Ln atoms. Thermogravimetric (TG) analysis showed that the N–C–P bonds are broken at temperatures above 400°C. A similar Pr complex was isolated as a finely crystalline powder and structurally characterized by the Rietveld method [25]. The crystal structure of a Nd complex with a similar structure was also studied in [26]. The complex $[Na(H_2O)_6]_2[LaNa_6H(H_2O)_{10}\{NTP\}_2] \cdot 3H_2O$ was isolated in a single-crystalline state and investigated [27]. In this complex, the

La^{3+} ion is encapsulated into a cage formed by two NTP molecules connected by inorganic P–O–Na–O–P bridges. It appears pertinent to make an attempt to synthesize an isomorphous series of crystals with La being replaced by other lanthanides and to study their structural features.

In this communication, we describe the synthesis and structure of the complexes $[Na(H_2O)_x]_2[Ln^{III}Na_6H(H_2O)_{10}\{N(CH_2PO_3)_3\}_2] \cdot nH_2O$, where Ln^{III} = Pr, Nd.

EXPERIMENTAL

Synthesis of I. The hydroxide of the appropriate lanthanide, freshly precipitated by reagent grade NaOH (0.006 mol, 0.24 g) from a solution of reagent grade $Ln(NO_3)_3 \cdot 6H_2O$ (0.001 mol, 0.44 g) and washed with water to a neutral pH, was added to an aqueous solution of NTP (twice recrystallized) (0.002 mol, 0.600 g) and reagent grade NaOH (0.008 mol, 0.320 g). The reaction mixture was stirred until a homogeneous transparent solution formed (pH 8.8–9.2) and filtered. Slow evaporation of the solvent gave crystals as light green (complex **I**) or reddish-violet (complex **II**) monoclinic prisms of platelike habit. The crystals were washed with a 45% aqueous solution of ethanol and then with diethyl ether, and dried at room temperature. The yields were 0.92 g (65%) for complex **I** and 0.84 g (59%) for complex **II**.

The quantitative determination of lanthanides was performed according to GOST 10398-76, and the total phosphorus was quantified according to PND F 14.1:4.248-07.

For **I**,		
Anal. calcd., %	Pr, 9.95	P, 13.12
Found, %	Pr, 10.1 ± 0.4	P, 13.0 ± 0.2
For **II**,		
Anal. calcd., %	Nd, 10.16	P, 13.09
Found, %	Nd, 10.3 ± 0.4	P, 13.2 ± 0.2

X-ray diffraction. The primary fragments of structures **I** and **II** were identified by direct methods, the atomic positions were derived from difference electron density maps. The nonhydrogen atom parameters were refined in the anisotropic approximation by the least squares method on $|F|^2$. The H atom positions were refined in the isotropic approximation, with constraints being imposed upon some H atoms. The protons of disordered water molecules could not be located. The crystallographic characteristics, X-ray diffraction experiment details, and structure refinement details are summarized in Table 1. Selected bond lengths and bond angles of structures **I** and **II** are presented in Table 2.

The X-ray diffraction data are deposited with the Cambridge Crystallographic Data Centre (CCDC nos. 1825702 (**I**) and 1825700 (**II**); deposit@ccdc.cam.ac.uk or http://www.ccdc.cam.ac.uk/data_request/cif).

Thermogravimetric analysis of **I** and **II** was carried out on a Shimadzu DTG-60H automated diffractometer in the 30–500°C range at a heating rate of 3°C/min under argon. Powder X-ray diffraction analysis of the products of thermal decomposition of **I** and **II** was performed on a DRON-6 two-circle diffractometer with CoK_α radiation (λ = 1.79026 Å) in the range 2θ = 6°–100°. The IR spectra of **I** and **II** and products of their thermal decomposition were measured in KBr pellets on an FSM-1201 Fourier transform spectrometer in the range of 450–5000 cm^{-1}. The UV/Vis spectra of aqueous solutions of **I** and **II** and products of their thermal decomposition were recorded in KBr pellets on an FSM-1201 Fourier transform spectrometer in the range of 450–5000 cm^{-1}. The Raman spectra of the single crystals **I** and **II** were run on a Centaur U-HR microscope microspectrometer in the 475–575 nm range with laser excitation at 473 nm.

RESULTS AND DISCUSSION

The structure of Ln coordination sphere in **I** and **II** (Fig. 1a) is similar to that described previously for La complex [27]. The lanthanide atom located at the inversion centers is encapsulated inside a cage composed of two NTP molecules connected by six inorganic P–O–Na–O–P bridges. The axis connecting the nitrogen atoms of the NTP molecules passes through the lanthanide atom, and the ligand molecules are rotated relative to each other through 60°.

The Ln atom is coordinated to two NTP nitrogen atoms and six oxygen atoms. The presence of Ln–N bonds is confirmed by the fact that bond angles at the nitrogen atoms are close to tetrahedral angles, indicating quaternization of nitrogen with the Lewis electron pair being involved in the chemical bond. In each PO_3 group, one oxygen atom coordinates both lanthanide and sodium atoms, one more oxygen coordinates only Na, and the third oxygen is hydrogen-bonded to water molecules. All oxygen atoms of the PO_3 groups are protonated, as indicated by the P–O distances (1.520(4)–1.5426(16) Å). As shown by structure analysis of other phosphonate complexes, the protonation of O atom increases the P–O distance by ~0.06 Å [12–18, 22, 27] due to displacement of the electron density towards the proton. However, the P–O distances are somewhat longer (on average, by 0.014(4) Å) for the oxygen atoms bound to Ln than for other PO_3-group oxygen atoms. This attests to noticeable participation of the oxygen electron density in the formation of Ln–O bonds, which thus contains a certain covalent contribution, unlike the typical ionic Na–O bond.

Each of the Na(1)–Na(3) ions contained in the $[LnNa_6H(H_2O)_{10}\{N(CH_2PO_3)_3\}_2]^{2-}$ complex anion is

Table 1. Crystallographic characteristics and X-ray experiment and structure refinement details for **I** and **II**

Parameter	Value	
	I	**II**
Molecular formula	$C_6H_{69}N_2O_{46}P_6Na_8Pr$	$C_6H_{69}N_2O_{46}P_6Na_8Nd$
M	1416.26	1419.60
System, space group, Z	Monoclinic, $P2_1/c$, 2	
a, Å	11.8168(7)	11.7999(2)
b, Å	10.5403(9)	10.5495(2)
c, Å	19.8094(10)	19.7976(3)
β, deg	94.232(5)	94.158(2)
V, Å ^{3}	2460.6(3)	2457.98(7)
ρ(calcd.), g/cm ^{3}	1.866	1.894
Radiation; λ, Å	MoK_α; 0.71073	
μ, mm^{-1}	1.375	1.442
T, K	100(1)	
Crystal size, mm	0.94 × 0.52 × 0.59	0.54 × 0.33 × 0.20
Diffractometer	XtaLAB Pro MM003, PILATUS 200K	
Scan mode	ω	
Absorption corrections	Analytical [28]	
T_{min}/T_{max}	0.336/0.458	0.482/0.770
$\theta_{min}/\theta_{max}$, deg	3.648/34.103	3.462/32.996
Ranges of indices h, k, l	$-16 \le h \le 18$, $-12 \le k \le 15$, $-31 \le l \le 30$	$-17 \le h \le 17$, $-16 \le k \le 15$, $-30 \le l \le 29$
Numbers of reflections: measured/unique (N_1) (R_{Int})	34 979/8625 (0.075)	77 711/8622 (0.033)
Numbers of reflections with $I > 2\sigma(I)$ (N_2)	7516	8000
Method of refinement	Full-matrix least squares on F^2	
Number of parameters/constraints	349/3	354/3
S	1.125	1.057
R_1/wR_1 for N_1	0.083/0.1659	0.037/0.0807
R_1/wR_1 for N_2	0.0733/0.1625	0.0339/0.0794
$\Delta\rho_{min}/\Delta\rho_{max}$, e/Å^3	−1.897/2.693	−0.974/2.014
Programs	CrysAlisPro [29], SHELX-2014 [30], WinGX [31], VESTA 3.0 [32]	

coordinated by two oxygen atoms of the PO_3 group of one NTP molecule and one oxygen atom of the PO_3 group of the other NTP molecule, which thus occupies the bridging position. Three more meridional positions in the coordination sphere of each Na^+ ion are occupied by water molecules.

The formation of the complex anion is accompanied by closure of chelate rings including six five-membered Ln–N–C–P–O rings with common Ln–N bonds, six eight-membered Ln–O–P–C–N–C–P–O rings, and six four-membered P–O–Na–O rings. Altogether, the NTP molecule coordinates seven metal atoms.

The average Ln–O distance (2.423(12) Å for Ln = Pr and 2.407(11) Å for Ln = Nd) is considerably shorter than the sum of the covalent radii [33] (r_C(Pr) = 2.03(7), r_C(Nd) = 2.01(6), r_C(O) = 0.66(2) Å). This is evidently attributable to the formation of multiple Ln⋯O coordination bond. The La–N distances of complexes **I** and **II** (2.986(4) and 2.9728(16) Å,

Table 2. Selected interatomic distances (*d*), bond angles (ω), and torsion angles (θ) in structures **I** and **II**

Bond	*d*, Å	
	I	**II**
Ln–N	2.986(4)	2.9728(16)
Ln–O	2.408(3)–2.438(4)	2.3922(13)–2.4193(15)
N–C	1.462(7)–1.485(6)	1.473(3)–1.484(2)
C–P	1.813(6)–1.825(5)	1.816(2)–1.820(2)
P–O	1.520(4)–1.530(3)	1.5223(17)–1.5301(17)
P–O(Ln)	1.540(3)–1.542(4)	1.5383(14)–1.5407(14)
Na(1)–O	2.391(5)–2.589(4)	2.3808(18)–2.585(2)
Na(2)–O	2.391(4)–2.526(4)	2.386(2)–2.5837(17)
Na(3)–O	2.380(5)–2.580(6)	2.3748(18)–2.5194(17)
Na(4)–O	2.160(17)–2.980(14)	2.156(7)–2.985(6)
Angle	ω, deg	
NLnO	63.71(11)–64.75(11)	63.79(5)–64.73(4)
	115.25(11)–116.29(11)	115.27(4)–116.21(5)
OLnO	100.85(12)–103.16(12)	100.98(5)–103.19(5)
CNLn	108.1(3)–109.0(3)	108.44(10)–108.88(11)
CNC	109.9(4)–110.7(4)	110.11(15)–110.41(14)
OPC	104.1(2)–110.0(2)	103.80(9)–110.13(9)
OPO	110.1(2)–113.5(2)	110.40(8)–113.33(8)
ONa(1)O	131.06(13)–162.42(19)	132.18(6)–161.33(6)
	73.98(13)–124.39(16)	60.44(5)–122.75(6)
ONa(2)O	133.51(15)–157.76(16)	130.63(5)–162.98(8)
	60.77(13)–127.91(15)	58.54(5)–124.70(7)
ONa(3)O	132.72(15)–161.16(16)	132.98(6)–158.12(7)
	60.35(13)–122.35(15)	61.00(5)–128.47(6)
ONa(4)O	15.2(3)–174.3(2)	12.59(19)–174.96(8)
Angle	θ, deg	
LnNCP	42.45(5)–43.69(5)	42.06(4)–43.73(4)

respectively) are significantly longer than the sum of the Ln and N covalent radii [33]. The differences between the M–N and M–O distances for complexes **I** and **II** are 0.562(16) and 0.565(13) Å, respectively.

In order to estimate the geometric configuration of the coordination polyhedra (CP) of the metal ions contained in the $[LnNa_6H(H_2O)_{10}\{N(CH_2PO_3)_3\}_2]^{2-}$ complex anion, the degree of similarity $\Phi(T,S)$ was calculated for the experimentally identified CP (*T*) and the reference polyhedron (*S*) by the procedure described in detail in [16, 34]. The calculations were carried out by the Polyhedron program of the Pseudo-Symmetry package (http://phys.unn.ru/ps) with the sensitivity parameter $\lambda = 1.1914$ rad^{-1}. Representing the lanthanide CP $[LnN_2O_6]$ as a distorted hexagonal bipyramid leads to the degree of similarity $\Phi_{Pr, Nd} \approx 0.05$. The highest similarity ($\Phi_{Pr, Nd} \approx 0.58$) is attained when the CP $[LnN_2O_6]$ in compounds **I** and **II** is described as a rhombohedron (Table 3). Rhombohedron is a distorted cube extended along the body diagonal. Each rhombohedron face is a rhombus extended along one diagonal. For complex **I**, the rhombohedron edge is 2.96(6) Å and the face diagonals are 3.77(4) and 4.60(2) Å; for **II**, the edge is 2.97(7) Å and the face diagonals are 3.75(3) and 4.57(2) Å. The rhombohedral coordination is rare for lanthanides, which are usually coordinated in asymmetric 9–12-vertex polyhedral configurations. The $[NaO_6]$ coordination polyhedron (Fig. 1b) can be considered as a trigonal prism ($\Phi_{Na} \approx 0.10$–0.13) or octahedron twisted around the threefold axis ($\Phi_{Na} \approx 0.08$).

The crystal packing of complexes **I** and **II** is depicted in Fig. 2. The structure comprises layers (Fig. 2a) alternating along the *a* axis.

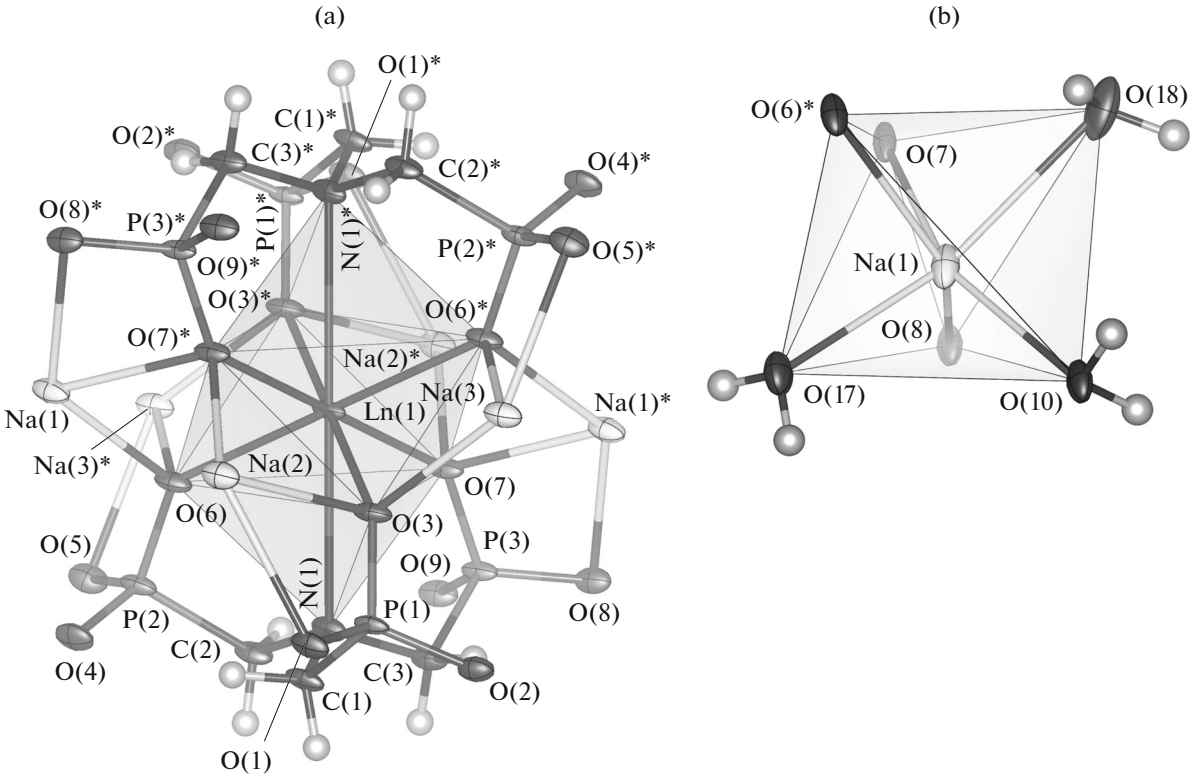

Fig. 1. Coordination polyhedra of metals contained in the $[LnNa_6H(H_2O)_{10}\{N(CH_2PO_3)_3\}_2]^{2-}$complex ion: (a) Ln, (b) Na^+ (for Na(1) atom; the polyhedra of Na(2) and Na(3) are similar). Symmetry codes: * $-x, -y, -z$.

These layers, located in (100) planes, are composed of the $[LnNa_6H(H_2O)_{10}\{N(CH_2PO_3)_3\}_2]^{2-}$ complex anions. Their structures are identical for complexes **I** and **II** and represent ribbons stretched along the *b* axis in which the complex anions are connected to one another by bridging O(13) water molecules (Fig. 2b). Each ribbon is tilted relative to the (100) plane; hence, each layer of the anions is corrugated.

The layers located in the (200) planes contain the $[Na(H_2O)_x]^+$ complex cations and solvate water molecules arranged in the voids between the cations. The structures of these layers differ for complexes **I** and **II** (Fig. 2c). The positions of water molecules in the

Table 3. Degrees of similarity (Φ) of the coordination polyhedra for structures **I** and **II**

Atom, C.N.	Trigonal prism	Cubic octahedron	Hexagonal bipyramid	Rhombohedron
		I		
Na(1), 6	**0.10014(18)**	0.07860(18)		
Na(2), 6	**0.1302(2)**	0.08211(18)		
Na(3), 6	**0.10285(19)**	0.08544(19)		
Pr(1), 6	0.02939(17)	**0.2782(2)**		
Pr(1), 8			0.05297(17) $c/a \approx 1.11$	**0.5823(4)** $c/a \approx 1.21$
		II		
Na(1), 6	**0.10024(17)**	0.08331(17)		
Na(2), 6	**0.09943(17)**	0.07919(17)		
Na(3), 6	**0.13209(17)**	0.08399(17)		
Nd(1), 6	0.02268(17)	**0.27653(18)**		
Nd(1), 8			0.05276(17) $c/a \approx 1.11$	**0.5780(2)** $c/a \approx 1.18$

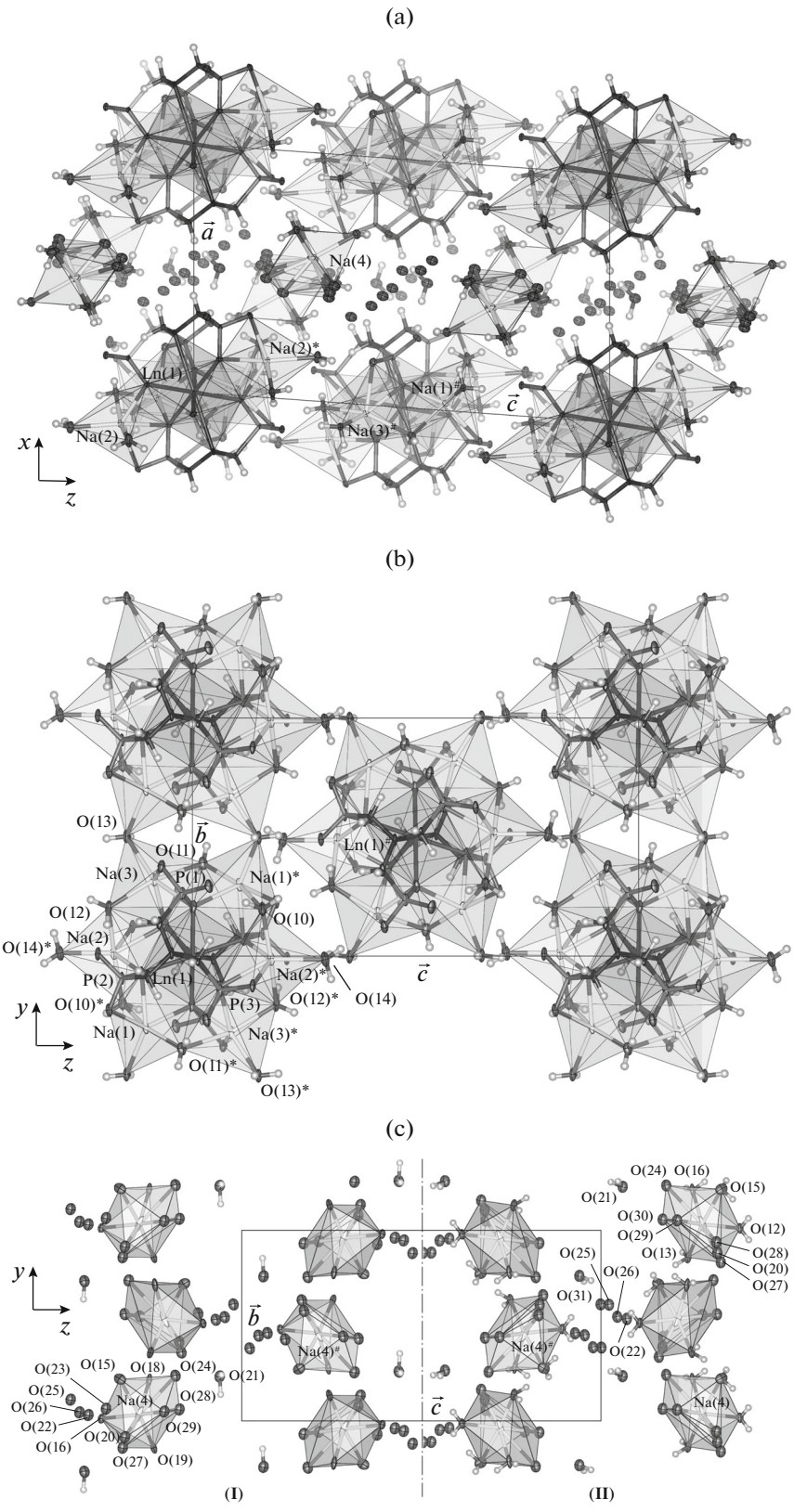

Fig. 2. Crystal packing of **I** and **II**: (a) layered packing projected onto the (101) plane; (b) (100) layer; (c) fragments of the (200) layer for complexes **I** and **II**. Symmetry codes: * $-x, -y, -z$; # $x, -y - 1/2, z - 1/2$.

(200) layers are highly disordered. This brings about certain ambiguity of the formal description of the complexes. The number of water molecules x that are conventionally included in the coordination sphere of the Na(4) ion and the number of solvate water molecules n depend on the choice of the limiting length for the Na–OH_2 coordination bond, which is quite arbitrary. The x and n values for structures **I** and **II** at the limiting Na–OH_2 bond length (taken to be 3 Å) are presented below:

Structure	x	n	$2x + n$
I	6.527	4.948	18.002
II	6.561	4.878	18.000

The conventional identification of the Na(4) coordination sphere in which most of positions of water molecules have non-integer populations makes analysis of the CP geometry for Na(4) inexpedient. The water molecules in **I** and **II** are connected to each other and to phosphonate oxygen atoms through hydrogen bonds. However, due to considerable disorder of water molecules, we were unable to locate most of hydrogen atoms and hydrogen bonds.

The UV/Vis spectra of complexes **I** and **II** in aqueous solutions (Fig. 3) are typical of triply charged lanthanide ions. The spectrum of complex **I** contains lines for Pr^{3+} transitions (the ground state term is $^3H_0$) to the states ^3P (423, 468, and 481 nm) and $^1D_2$ (583 nm) [35]. The UV/Vis spectrum of **II** shows Nd^{3+} transitions (the ground state term is $^4I_{9/2}$) to the states ^4D (unresolved multiplet at 347–359 nm), ^2D (427 and 461 nm), ^4G (475, 511, 524, and 582 nm), ^2G (511 and 582 nm), $^2H_{11/2}$ (526 nm), ^4F (682, 736, 803, and 872 nm), and $^4S_{3/2}$ (745 nm) [36].

The molecular vibrational spectra (Fig. 4) of complexes **I** and **II** are similar. The 150–230, 270, and 350 cm^{-1} groups of bands refer to vibrations of the complex ions as a whole; the differences between the spectra of complexes **I** and **II** in this range correspond to differences in the structures of the $[Na(H_2O)_x]^+$ complex ions. The broad band at 390–430 cm^{-1} and the group of bands at about 490, 520, 560, 580, and 620 cm^{-1} correspond to the δ(O–P–O(M)) vibrational modes in the coordination environment of metal ions. The high symmetry of the $[Ln^{III}Na_6H(H_2O)_{10}\{N(CH_2PO_3)_3\}_2]^{2-}$ complex ion is manifested as the alternative activity of most of these vibrational modes. The bands at 700–920 cm^{-1} refer to the N–C–P vibrations in the complex anion. The frequencies of about 720, 750, and 770 cm^{-1}, active only in the Raman spectra, refer to symmetric modes, and the 790, 850, and 910 cm^{-1} frequencies, which do not obey the alternative selection rule, correspond to asymmetric vibrational modes. The ν(P–O) vibrations give rise to alternative IR-active 970, 990, 1050,

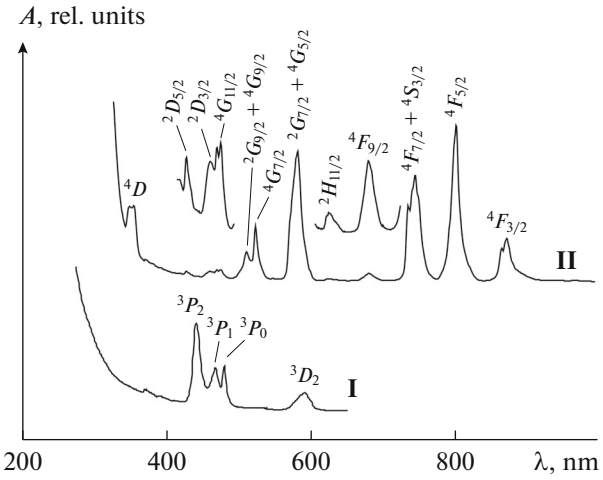

Fig. 3. UV/Vis spectra of 1% aqueous solutions of complexes **I** and **II** (absorbance A as a function of the wavelength λ).

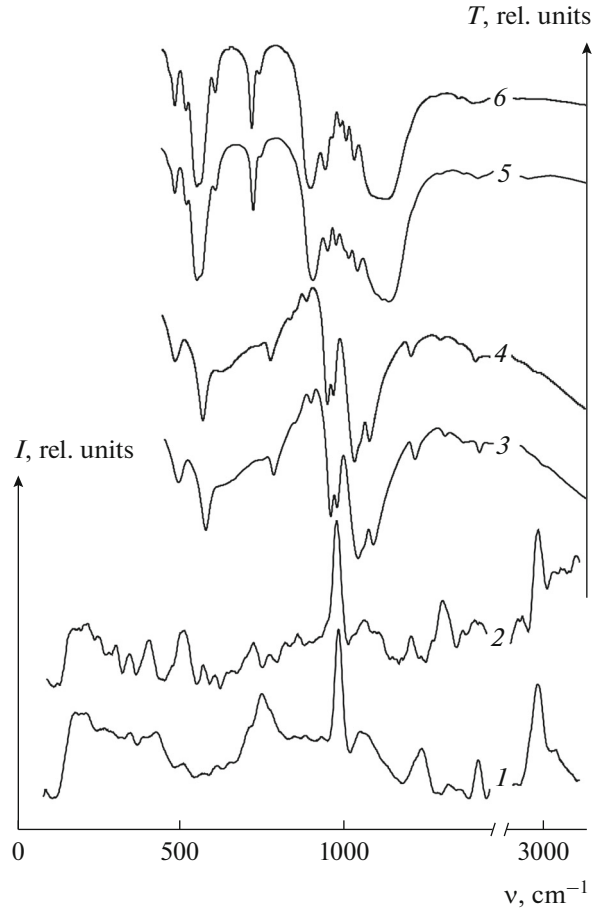

Fig. 4. Raman spectra (intensity I as a function of the wavenumber ν) of the single crystals of complexes (*1*) **I**, (*2*) **II**; IR spectra (transmittance T as a function of the wavenumber ν) of complexes (*3*) **I**, (*4*) **II**, and products of thermal decomposition under argon of complexes (*5*) **I** and (*6*) **II**.

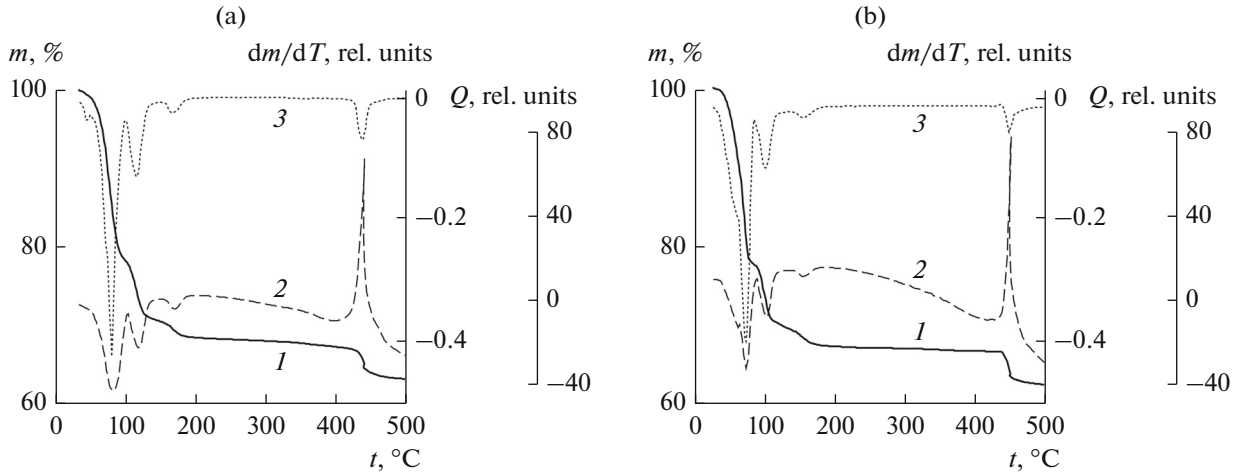

Fig. 5. Thermogravimetric curves of (a) **I**, (b) **II** under argon: (*1*) sample mass *m*, (*2*) heat *Q*, and (*3*) derivative d*m*/d*T* (*3*) as a function of temperature *T*.

and 1110 cm^{-1} bands and Raman-active 1000, 1070, and 1150 cm^{-1} bands. The vibrations of the localized P–O π-bond (~1250 cm^{-1}) give rise to strong Raman bands and weak IR bands. The other observable bands are (cm^{-1}): 1430 $\delta(CH_2)$, 1500–1600 $\delta(H_2O)$, 2950–2980 $\nu(CH_2)$.

Thermal decomposition of **I** and **II** under argon includes several steps (Fig. 5). In the 40–180°C range, water molecules are eliminated with endothermal effects. Because of the intricate structure of the complexes, the dehydration includes several steps: 30–100°C ($-19H_2O$), 100–130°C ($-7H_2O$), and 150–180°C ($-2H_2O$). On further heating up to 410°C, no other effects are manifested. In the 410–470°C range, mass loss of the sample takes place, which corresponded to elimination of the N_2 molecule and two H_2O molecules with a pronounced exothermic effect; this is consistent with the destruction of the N–C–P skeleton above 400°C noted in [24]. The IR spectra of the thermal decomposition products (Fig. 4, *5, 6*) show bands for sodium metaphosphate $NaPO_3$ [37, 38] (cm^{-1}: 485, 525 δ(O–P–O), 1010, 1030, 1060, 1110–1150 $\nu(PO_3)$) and bands similar to lanthanum orthophosphate $LnPO_4$ [39, 40] (cm^{-1}: 555, 570, 620, 730 δ(O–P–O), 960, 990, 1060 $\nu(PO_3)$). Powder X-ray diffraction analysis of decomposition products of **I** and **II** indicates the presence of monazite ($LnPO_4$, space group $P2_1/n$) [41].

ACKNOWLEDGMENTS

This work was performed as a basic part of the State Order to Higher Educational Institutions and Scientific Organizations for Research (project no. 3.6502.2017/BCh).

REFERENCES

1. *Koordinatsionnaya khimiya redkozemel'nykh elementov* (Coordination Chemistry of Rare Earth Elements), Spitsyn, V.I., and Martynenko, L.I., Eds., Moscow: MGU, 1979.
2. *Comprehensive Coordination Chemistry*, Wilkinson, G., Gillard, R.D., and McCleverty, J.A., Eds., Pergamon Press, 1987, vol. 3.
3. *Comprehensive Coordination Chemistry II*, McCleverty, J.A. and Meyer, T.J., Eds., Elsevier, 2003, vol. 3.
4. *Rare Earth Coordination Chemistry. Fundamentals and Applications*, Chunhui, H., Ed., New York: Wiley, 2010.
5. Porai-Koshits, M.A., Polynova, T.N., and Shkol'nikova, L.M., *Zhurn. Vyssh. Khim. Ob-va im. D.I. Mendeleeva*, 1984, vol. 29, no. 3, p. 43.
6. Stezowski, J.J. and Hoard, J., *Isr. J. Chem.*, 1984, vol. 24, p. 323. doi 10.1002/ijch.198400055
7. Schinzel, S., Bindl, M., Visseaux, M., and Chermette, H., *J. Phys. Chem. A*, 2006, vol. 110, p. 11324. doi 10.1021/jp060876d
8. Pearson, R.G., *J. Chem. Educ.*, 1999, vol. 76, no. 2, p. 267. doi 10.1021/ed076p267
9. Geerlings, P., De Proft, F., and Langenaeker, W., *Chem. Rev.*, 2003, vol. 103, no. 5, p. 1793. doi 10.1021/cr990029p
10. Cabeza, A., Ouyang, X., Sharma, C.V.K., et al., *Inorg. Chem.*, 2002, vol. 41, p. 2325. doi 10.1021/ic0110373
11. Demadis, K.D., Katarachia, S.D., and Koutmos, M., *Inorg. Chem. Commun.*, 2005, vol. 8, p. 254. doi 10.1016/j.inoche.2004.12.019
12. Somov, N.V. and Chausov, F.F., *Crystallogr. Rep.*, 2014, vol. 59, no. 1, p. 66. doi 10.1134/S1063774513050118
13. Somov, N.V. and Chausov, F.F., *Crystallogr. Rep.*, 2015, vol. 60, no. 2, p. 210. doi 10.1134/S1063774515010228
14. Somov, N.V., Chausov, F.F., Zakirova, R.M., and Fedotova, I.V., *Crystallogr. Rep.*, 2016, vol. 61, no. 2, p. 216. doi 10.1134/S1063774516020243

15. Somov, N.V., Chausov, F.F., Zakirova, R.M., and Fedotova, I.V. *Russ. J. Coord. Chem*., 2015, vol. 41, no. 12, p. 798. doi 10.1134/S1070328415110081
16. Somov, N.V., Chausov, F.F., and Zakirova, R.M., *Cryst. Rep*., 2017, vol. 62, no. 6, p. 857. doi 10.1134/S1063774517050224
17. Somov, N.V., Chausov, F.F., Lomova, N.V., et al, *Russ. J. Coord. Chem*., 2017, vol. 43, no. 9, p. 583. doi 10.1134/S1070328417090093
18. Somov, F.F., Chausov, R.M., Zakirova, I.V., et al., *Russ. J. Coord. Chem*., 2017, vol. 43, no. 12, p. 864. doi 10.1134/S1070328417120090
19. Kuznetsov, Yu.I., *Usp. Khim.*, 2004, vol. 73, no. 1, p. 79.
20. Chausov, F.F., Shabanova, I.N., Kazantseva, I.S., and Naimushina, E.A., *Izv. Akad. Nauk. Ser. Fiz.*, 2014, vol. 78. no. 4, p. 436.
21. Shabanova, I.N., Chausov, F.F., Naimushina, E.A., and Somov, N.V., *Surf. Interface Anal.*, 2014, vol. 46, p. 750. doi 10.1002/sia.5479
22. Somov, N.V. and Chausov, F.F., *Crystallogr. Rep.*, 2016, vol. 61, p. 39. doi 10.1134/S1063774516010235
23. Bazaga-García, M., Angeli, G.K., Papathanasiou, K.E., et al., *Inorg. Chem*., 2016, vol. 55, p. 7414. doi 10.1021/acs.inorgchem.6b00570
24. Tananaev, I.V., Tereshin, G.S., Kuznetsova, O.B., et al., *Zh. Neorg. Khim*., 1981, vol. 26. no. 1, p. 276.
25. Cunha-Silva, L., Mafra, L., Ananias, D., et al., *Chem. Mater.*, 2007, vol. 19, p. 3527. doi 10.1021/cm070596q
26. Beresnev, E.N., Kuznetsova, O.B., and Kop'eva, M.A., *Russ. J. Inorg. Chem*., 2009, vol. 54, no. 7, p. 1023. doi 10.1134/S0036023609070067
27. Somov, N.V., Chausov, F.F., Zakirova, R.M., et al., *Russ. J. Coord. Chem.*, 2017, vol. 42, p. 373. doi 0.1134/S1070328417060082
28. Clark, R.C. and Reid, J.S., *Acta Crystallogr., Sect. A: Found. Crystallogr.*, 1995, vol. 51, p. 887. doi 10.1107/S0108767395007367
29. *CrysAlisPro. Version 1.171.38.41*, Rigaku Oxford Diffraction, 2015.
30. Sheldrick, G.M., *Acta Crystallogr., Sect. A: Found. Crystallogr.,* 2008, vol. 64, p. 112. doi 10.1107/S0108767307043930
31. Farrugia, L.J., *J. Appl. Crystallogr.*, 1999, vol. 32, p. 837. doi 10.1107/S0021889899006020
32. Momma, K. and Izumi, F., *J. Appl. Crystallogr.*, 2011, vol. 44, p. 1272. doi 10.1107/S0021889811038970
33. Cordero, B., Gómez, V., Platero-Prats, A.E., et al., *Dalton Trans.*, 2008, no. 21, p. 2832. doi 10.1039/b801115j
34. Somov, N.V. and Andreev, P.V., *Crystallogr. Rep.*, 2018, vol. 63, no. 1, p. 32. doi 10.1134/S1063774518010170
35. Cai, Z., Umar, V.M., and Fischer, C.F., *Phys. Rev. Lett.*, 1992, vol. 68, p. 297. doi 10.1103/PhysRevLett.68.297
36. Wyart, J.-F., Meftah, A., Bachelier, A., et al., *J. Phys. B,* 2006, vol. 39, p. L77. doi 10.1088/0953-4075/39/5/L01
37. Ogden, J.S. and Williams, S.J., *J. Chem. Phys.*, 1980, vol. 73, no. 4, p. 2007.
38. Bencivenni, L. and Gingerich, K.A., *J. Mol. Struct.*, 1983, vol. 98, p. 195.
39. Savchyn, P., Karbovnyk, I., Vistovskyy, V., et al., *J. Appl. Phys.*, 2012, vol. 112, p. 124309.
40. Patil, Y.S., Chaudhari, K.G., Murthy, K.V.R., and Poornachandra Rao, N.V., *Arch. Appl. Sci. Res.*, 2012, vol. 4, no. 2, p. 757.
41. Ni, Y., Hughes, J.M., and Mariano, A.N., *Am. Mineral.*, 1995, vol. 80, p. 21.

Translated by Z. Svitanko